On the other hand, observations in the solid state for hard degrees of freedom are likely to be representative of solution structure as well.

It also seems worth noting that conformational analysis of a system as complex as $XM(PR_3)_3$ and with the amount of detail given above would be difficult to achieve by molecular mechanics calculations. The main difficulty is a lack of appropriate potential functions.

One might ask what conclusions can be drawn, from our analysis, about the catalytic activity of $ClRh(PPh_3)_3$[46] and related compounds. One possible answer would be: there are no direct conclusions, because, as has been shown in the last few years,[47] the catalytically active species is $ClRh(PPh_3)_2$ with one PPh_3 dissociated and not $ClRh(PPh_3)_3$. Another answer relates to catalysts for asymmetric hydrogenation[48] and related reactions. Consider the complexes **19** of chiraphos as an example. The basic asymmetry is located on the carbon atoms of the five-membered chelate ring. In order to induce asymmetry in hydrogenations, it must be transmitted to the opposite side of the Rh complex. It has been argued[49] that it is the phenyl groups on phosphorus that act as transmitters of asymmetry. Our analysis has certainly shown that it is possible to transmit information from one side of a Rh complex to the other ($P1R_3$ to $P3R_3$), that the mechanism of transmission may be based on nonbonded interactions, and that there is not necessarily a unique transmission of information (path 1 and path 2). So far we have not considered the role of the phenyl groups themselves, but it is known[2a] that triphenylphosphine shows certain preferred patterns of conformation. We are presently investigating how these patterns might combine with the conformation of the PR_3 groups in compounds of the type $XYM(PPh_3)_2$ and what the stereochemical consequences are if the two phosphine ligands are linked by an ethylene bridge as is the case for the ligand chiraphos (**19**).

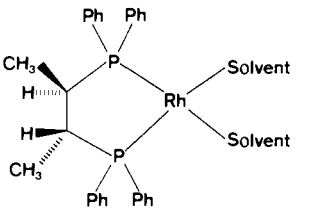

19

Acknowledgment. This work was supported by the Schweizerischer Nationalfonds zur Förderung der wissenschaftlichen Forschung.

Registry No. 1, 57810-25-0; **2**, 67426-13-5; **3**, 68664-86-8; **4**, 52242-35-0; **5**, 72778-75-7; **6**, 77700-88-0; **8**, 56954-48-4; **9**, 71357-03-4; **10**, 60364-00-3; **12**, 14694-95-2; **13**, 36103-64-7; **14**, 39248-25-4.

Supplementary Material Available: Appendix deriving eq 13 and 14 from eq 11 and 12 (5 pages). Ordering information is given on any current masthead page.

(46) Osborn, J. A.; Jardine, F. H.; Young, J. F.; Wilkinson, G. *J. Chem. Soc. A* **1966**, 1711.
(47) For a summary of the mechanism of catalysis see: Halpern, J. *Inorg. Chim. Acta* **1981**, *50*, 11.
(48) For a summary of the mechanism of asymmetric hydrogenation see: Halpern, J. *Science (Washington, D.C.)* **1982**, *217*, 401.
(49) Knowles, W. S.; Vineyard, B. D.; Sabacky, M. J.; Stults, B. R. In "Fundamental Research in Homogeneous Catalysis"; M. Tsutsui, Ed.; Plenum, New York, 1979; Vol. 3, 357.

Models for the Photosynthetic Water Oxidizing Enzyme. 2. Electronic, Magnetic, and EPR Characterization of a Binuclear Manganese(II) Semiquinone Complex

P. Mathur[†] and G. C. Dismukes*

Contribution from the Department of Chemistry, Princeton University, Princeton, New Jersey 08544. *Received May 3, 1982*

Abstract: The preparation and characterization of a tetranuclear manganese complex, $Mn_4(ASQ)_4(CO)_8$, and a binuclear complex into which it dissociates in solution, $Mn_2(ASQ)_4L_2$ (ASQ ≡ 2-acetyl-1,4-benzosemiquinone), is described. EPR spectroscopy and variable temperature magnetic susceptibility of the solution species indicate that there are two equivalent Mn(II) ions coupled by a ferromagnetic exchange interaction, having $J \geq 23$ cm^{-1}, fostered by two bridging semiquinones. This is evidenced by a paramagnetic ground state with a magnetic moment $\mu_{eff} = 6.78$, electron spin resonance fine structure consistent with an apparent spin $S = 3$ and having zero-field splitting parameters of $|D| = 0.103$ cm^{-1} and $|E| = 0.011$ cm^{-1}, a nearly isotropic 11-line hyperfine structure for ^{55}Mn with coupling constant $|A| = 45 \pm 3$ G, and a nearly isotropic $g = 2$. The quenching of the magnetic moment of the dimer with increasing temperature is interpreted to arise from the ferromagnetic coupling and, near room temperature, from an internal redox equilibrium in which $Mn_2(AQL)_4L_2$ and possibly $Mn_2(ASQ)_2(AQL)_2L_2$ (AQL ≡ 2-acetyl-1,4-benzoquinol dianion) form. This complex is discussed in relation to its suitability as a model for the magnetic properties of the photosynthetic water-oxidizing enzyme.

The mechanism by which green plats and algae oxidize water to molecular oxygen during photosynthesis is a poorly understood process. However, recent advances have established some clues on the identity of the active site of the metalloenzyme which mediates this important chemistry. This developing knowledge can now serve as a basis for the development of molecular models of the active site.[1,2]

EPR spectroscopic observation of the native enzyme in chloroplasts has shown that the active site consists of a binuclear, or possibly tetranuclear, manganese cluster.[3] Characterization of the manganese hyperfine structure, by comparison with mixed-valence binuclear Mn model compounds, has shown that Mn(III)

[†] Current Address: Ramjas College, Delhi University, Delhi, India.

(1) Cooper, S. R.; Dismukes, G. C.; Klein, M.; Calvin, M. *J. Am. Chem. Soc.* **1978**, *100*, 7248.
(2) Unni Nair, B. C.; Dismukes, G. C. *J. Am. Chem. Soc.* **1983**, *105*, 124.
(3) Dismukes, G. C.; Siderer, Y. *FEBS Lett.* **1980**, 121.

0002-7863/83/1505-7093$01.50/0 © 1983 American Chemical Society

and Mn(IV) oxidation states are present in a deeply trapped mixed-valence cluster.[4,5] A protein of molecular weight 34 kD has been implicated as the binding site for Mn[6-8] and has recently been observed to bind 2 Mn ions that are electronically coupled.[9] Although the stoichiometry for Mn requirement in O_2 evolution in intact photosynthetic membranes is four,[10,11] it is not clear if one or two of these proteins are present, or if two Mn ions are catalytic and two are structural.[12]

There is indirect evidence implicating interaction between Mn and plastosemiquinone at the site of photosynthetic oxygen evolution.[13] A transient radical species identified as "quinoidal" in character has been found to exhibit altered electron spin relaxation upon treatments that release bound Mn.[13]

Several monomeric metal quinone complexes have been reported,[15-19] including a manganese(IV)tris(catecholate) complex.[20] Tetranuclear Co(II) and Ni(II) complexes have been reported with 3,5-di-*tert*-butyl-1,2-benzoquinone.[21]

Experimental Section

(a) 2-Acetyl-1,4-benzoquinone. The ligand was synthesized by oxidizing a sample of 2,5-dihydroxyacetophenone (Aldrich) with freshly precipitated silver oxide in dry, distilled benzene.[22]

(b) $Mn_4(ASQ)_4(CO)_8$·toluene. Dimanganese decacarbonyl (Sterm Chemical Co.; 0.39 g, 1 mmol) was photolyzed in a thermostated cell at 10–15 °C in the presence of 2-acetyl-1,4-benzoquinone (0.60 g, 4 mmol) in degassed, dried, distilled toluene under a steady flow of argon gas. The reaction mixture gradually turned dark green, depositing a deep green microcrystalline product. The reaction was stopped after 6 equiv of CO evolved. This material was washed with toluene under argon to remove excess quinone and manganese decacarbonyl. The same compound composition is obtained regardless of the stoichiometry of the reactants or the length of photolysis. Illumination of a free solution of the isolated quinone for the same interval of time yields minimal changes in the UV–vis region. Analytical data and infrared spectroscopy support the presence of 1 mol of toluene as solvate. Anal. Calcd for $C_{47}H_{32}O_{20}Mn_4$: C, 49.69; H, 2.84; O, 28.17; Mn, 19.37. Found: C, 49.41; H, 3.52; O, 27.77; Mn, 19.38. C, H, and O analyses were by Gailbraith Laboratory. Fast atom bombardment mass spectrometry of this material in thioglycerol established the presence of peaks at m/e 1044 and 1184, consistent with $Mn_4(SQ)_4(CO)_8$ and $Mn_4(SQ)_4(CO)_8$·thioglycerol, respectively. (These measurements were conducted at the NSF Regional Facility at Johns Hopkins University, Courtesy of Dr. R. J. Cotter.)

For the solution studies, this material was dissolved in acetonitrile or dimethoxyethane (DME) and filtered prior to use. Acetonitrile was freshly distilled and stored over degassed molecular sieve. DME was dried over sodium and degassed.

(c) Instrumentation. For the photolysis experiments the source of near-UV radiation was a merry-go-round Rayonet Model RPR-100 photochemical reactor equipped with sixteen 350-nm lamps. Sample cells were made of Pyrex glass. Identical results on one experiment were observed with use of a tungsten lamp filtered to cut off wavelengths longer than 350 nm.

All IR spectra were obtained with use of a PE-283 spectrophotometer. Electronic spectra were recorded on a HP 8450A UV/VIS spectrophotometer.

EPR spectra were obtained at X-band (9.23 GHz) on a Varian E-12 spectrometer with magnetic field modulation at 100 kHz. An Oxford helium cryostat maintained temperatures from 3.5 to 100 K. Frozen solutions of the complex in spectrograde, sodium-dried, distilled dimethoxyethane were examined in cylindrical quartz tubes. Flat EPR cells were used for fluid samples.

Magnetic susceptibility measurements were made with use of the Evans method[23] on a Varian XL-100 FTNMR spectrometer. The probe temperature was measured with use of calibrated, copper–constantan thermocouple. Diamagnetic corrections were applied by using Pascal's constants.[24]

An exhaustive electrolysis was carried out on a three-electrode assembly in a two-compartment cell with side-inlets for argon gas. A PAR-173 potentiostat was used for maintaining a constant potential of −0.6 V, SCE. Dried, freshly distilled acetonitrile was used as solvent. A ferrocene/ferrocenium couple was used as an internal standard.

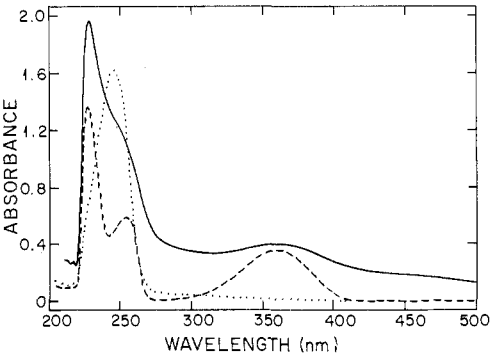

Figure 1. UV–vis spectra is acetonitrile: (—) 2-acetyl-1,4-benzosemiquinone–manganese(II,II) dimer at 8.3 μM, λ_{max}^{nm} 226, 246, 357, and 474 and log ϵ = 5.35, 5.16, 4.70, and 4.40, respectively; (···) 2-acetyl-1,4-benzoquinone, 11.4 μM; (---) 2-acetyl-1,4-benzoquinol, 11.4 μM.

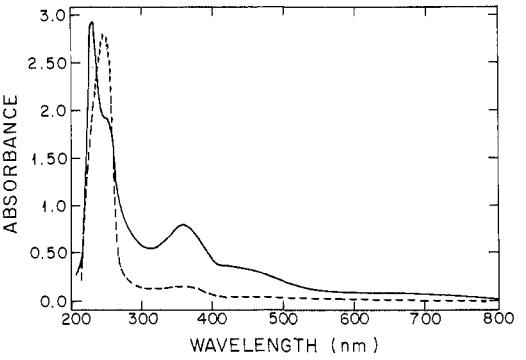

Figure 2. UV–vis spectra in acetonitrile: (—) 2-acetyl-1,4-benzosemiquinone, obtained by one-electron reduction of the quinone at a Pt electrode [λ_{max}^{nm} (log ϵ) = 227 (4.17), 246 (3.99), 3.57 (3.59), and 440 (2.18), conccentration 20 μM]; (---) 2-acetyl-1,4-benzoquinone, after reoxidation of the semiquinone.

Results

Electronic and Infrared Spectroscopy. The electronic spectrum of the manganese quinone complex in acetonitrile has three bands at λ_{max} 226, 246 and 357 nm; log ϵ = 5.35, 5.16 and 4.70; and a weak shoulder a 474 nm as shown in Figure 1. A comparison of the spectrum of the complex with that of the free quinone, the semiquinone anion, and the quinol shows that photolysis of dimanganese decacarbonyl is the presence of the ligand leads to reduction of the ligand.

(4) Dismukes, G. C.; Siderer, Y. *Proc. Natl. Acad. Sci. U.S.A.* **1981**, *78*, 274.
(5) Dismukes, G. C.; Ferris, K.; Watnick, P. *Photobiochem. Photobiophys.* **1982**, *3*, 243.
(6) Kuwabara, T.; Murata, N. *Plant Cell Physiol.* **1982**, *23*, 533–539.
(7) Yamamoto, Y.; Shjimada, S.; Nishimura, M. *FEBS Lett.* **1983**, *151*, 49–53.
(8) Bishop, N. I. In "The Oxygen Evolving System of Plant Photosynthesis"; Inoue, Y., Ed.; Academic Press: Tokyo 1983.
(9) Dismukes, G. C.; Abramowicz, D. A.; Ferris, K. F.; Mathur, P.; Siderer, Y.; Upadrashta, B.; Watnick, P. In "The Oxygen Evolving System of Plant Photosynthesis"; Inoue, Y., Ed.; Academic Press: Tokyo, 1983; p 141.
(10) Cheniae, G.; Martin, I. F. *Biochim. Biophy. Acta* **1970**, *197*, 252.
(11) Yocum, C. F.; Yerkes, C. T.; Blankenship, R. E.; Sharp, R. R.; Babcock, G. T. *Proc. Natl. Acad. Sci. U.S.A.* **1981**, *78*, 7507–7511.
(12) Klimov, V. V.; Allakhverdiev, S. I.; Shuvalov, V. A.; Krasnovsky, A. A. *FEBS Lett.* **1982**, *148*, 307–310.
(13) Nugent, J. H. A.; Evans, M. C. W.; Diner, B. A. *Biochim. Biophys. Acta* **1982**, *682*, 106.
(14) Warden, J. T.; Blankenship, R. E.; Sauer, K., *Biochim. Biophys. Acta* **1976**, *423*, 462.
(15) Rohrscheid, F.; Balch, A. L.; Holm, R. H. *Inorg. Chem.* **1966**, *5*, 154.
(16) Cenini, S.; Ugo, R.; Monica, G. *J. Chem. Soc. A* **1971**, 416.
(17) Girgis, A. Y.; Sohn, Y. S.; Balch, A. L. *Inorg. Chem.* **1975**, *14*, 2327.
(18) Pierpont, C. G.; Francesconi, L. C.; Hendrickson, D. N. *Inorg. Chem.* **1978**, *17*, 3470.
(19) Buchanan, R. M.; Kessel, S. L.; Downs, H. N.; Pierpont, C. G.; Hendrickson, D. N. *J. Am. Chem. Soc.* **1978**, *100*, 7874.
(20) Hartman, J. R.; Foxman, B. M.; Cooper, S. R. *Chem. Commun.* **1982**, 583.
(21) Buchanan, R. M.; Fitzgerald, B. J.; Pierpont, C. G. *Inorg. Chem.* **1979**, *18*, 3439.
(22) Kloetzel, M. L.; Dayton, R. P.; Abadir, B. Y. *J. Org. Chem.* **1955**, *20*, 47.
(23) Evans, D. F. *J. Chem. Soc.* **1959**, 2003.
(24) Mabbs, F. E.; Machin, D. J. "Magnetism and Transition Metal Ions"; Chapman and Hall, London, 1973.

It is also pertinent to observe that the 474-nm band in the complex is bleached upon oxygenation for 30 min, in contrast to 2-acetyl-1,4-benzoquinol which does not absorb in this region. However, when a trace of base is added to a solution of the free quinol, in order to generate the semiquinone anion by air oxidation,[25] a new shoulder appears at 430 nm, which also gets bleached upon extended oxygenation but not if purged with argon instead. This suggests that the oxidation state of the ligands in the complex is the semiquinone.

To ascertain the oxidation state of the ligand in the complex, we carried out a one-electron reduction of 2-acetyl-1,4-benzoquinone in degassed acetonitrile solution at a platinum electrode at a potential of −0.6 V, using dried *tert*-butylammonium perchlorate as a supporting electrolyte. After an exhaustive electrolysis, corresponding to one electron transferred per ligand molecule, an aliquot was transferred by an air-tight syringe to a degassed optical cell and the spectrum recorded. The semiquinone shows three prominent peaks at λ_{max} 227, 246, and 357 nm, log ϵ = 4.17, 3.99 and 3.59, and a weaker band at 440 nm, log ϵ = 2.18 (Figure 2). The band at 440 nm bleaches upon oxygenation, as was the case for the base-generated semiquinone. 2-Acetyl-1,4-benzoquinone shows a much weaker absorption around 450 nm, which is not sensitive to oxygenation and may be due to an impurity. We conclude from these data that the ligand adds oxidatively to a coordinately unsaturated manganese decarbonyl photoproduct and is reduced by one electron to form the semiquinone.

A typical infrared spectrum exhibits two distinct bands in the ν(C≡O) region at 2020 and 1919 cm^{-1}. Bands at similar positions are seen for inequivalent terminal carbonyls in tetramers like $[Re(CO)_3OH]_4$ and $[Mn(CO)_3OH]_4$.[26,27] These bands are stable in the solid product but disappear from DME solutions under argon over 1 day, indicating lability of the remaining CO's. The free quinone carbonyls and the side-chain keto groups occur at 2650 and 1710 cm^{-1}, respectively. These bands are lost in the reaction product and in their place a single band is observed at 1620 cm^{-1}. This is supporting evidence for coordination of the carbonyl groups at the metal center.

EPR Spectra. The EPR spectra for the parent solid complex and its solutions in DME or acetonitrile differ significantly. A weak, featureless, broad signal is observed in the solid at 4.2 K at an effective g of 2. As the temperature is increased the signal weakens and begins to narrow, suggesting the presence of intermolecular exchange narrowing.

By contrast, the EPR spectrum at 10.6 K of a frozen solution in DME exhibits a group of six fine structure peaks labeled III and centered at g = 2 (Figure 3a). These are flanked by three additional peaks, two of which appear at lower fields (I, III) and one at a higher field (IV). Superimposed on this fine structure, for the two low-field peaks in the cluster labeled III, can be resolved hyperfine structure as illustrated in Figure 3b. This hyperfine structure consists of 11 lines on each fine structure peak with a near integer intensity distribution of 1:2:3:4:5:6:5:4:3:2:1. The hyperfine coupling constant is nominally 45 ± 3G, which is close to half of the value found for monomeric Mn(II) complexes. This is compelling evidence for a pair of magnetically equivalent high-spin Mn(II) ions coupled by an electron spin exchange interaction.[28] The fine structure is consistent with a ground state having a spin $S \geq 2$ for this dimer. The product of (EPR height)(line width)^2(temperature)/(receiver gain) decreases monotonically with increasing temperature above 10 °K. This evidence indicates the presence of low-lying, EPR-silent, excited spin states that are populated as the temperature increases.

The central peak in the group (III) exhibits only six hyperfine lines with an average spacing of 85–80 G. This is typical of monomeric Mn(II) quinone complexes. The amplitude varies

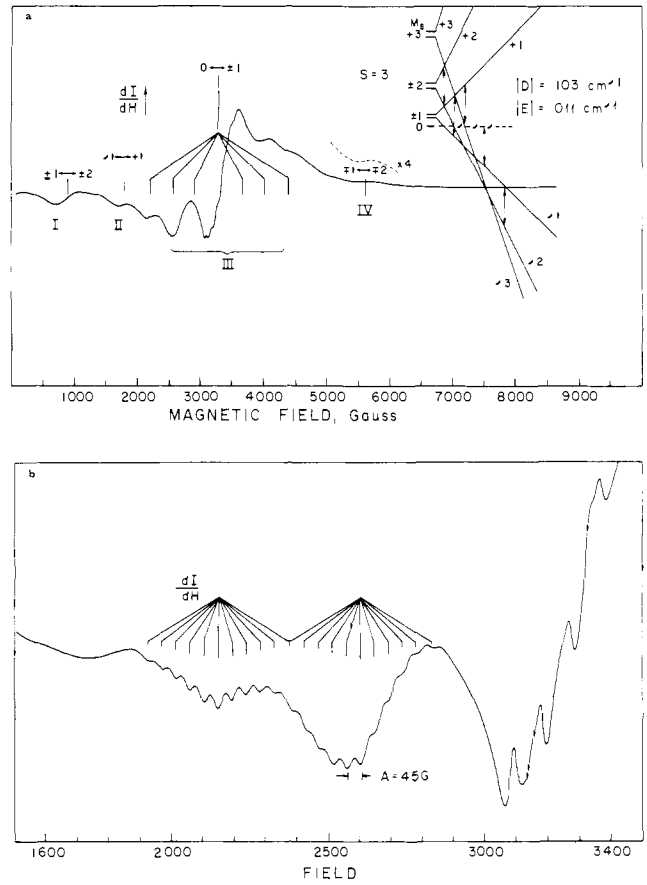

Figure 3. (a) EPR spectrum of 2-acetylbenzosemiquinone–manganese(II,II) dimer (10^{-3} M) in dimethoxyethane at T = 11 K. Microwave power 10.0 mW, microwave frequency 9.228 GHz, 25-G modulation amplitude. (b) A 2000-G scan of the manganese dimer centered at 2500 G, showing hyperfine structure.

relative to the other peaks in this group and is suppressed by minimizing exposure to air and to elevated temperatures. Evidently it is due to monomeric Mn(II) arising from equilibrium dissociation or air oxidation of the dimer. Attempts at purification by recrystallization have failed to completely remove this feature. A quantitative comparison to the dimer intensity is complicated by the population of low-lying spin states in the dimer and the monomer. We estimate less than 3% contribution by monomer from the ratio of integrated areas.

Magnetic Behavior. Two variable temperature magnetic susceptibility studies on the isolated solid product were conducted with use of a modified Princeton Applied Research vibrating sample magnetometer (measurements courtesy of Dr. V. Petrouleas, Nuclear Research Center, "Demokritos", Athens, Greece). Because of a suspected oxidation during shipping, the two samples studied did not show the same absolute values, but were consistent in establishing a clear quenching of the magnetic moment at lower temperatures: μ_{eff} = 8.10, 7.51, 4.89 ± 0.51 at 297, 70.5, and 1.71 K, respectively. μ_{eff} is in Bohr magnetons per $Mn_4(ASQ)_4(CO)_8$·toluene (M_r = 1136).

The solution magnetic susceptibility of the complex was determined in spectrograde acetone over the temperature range 198 to 294 K. The average molar susceptibility (χ) corrected for diamagnetism of ligand atoms is given in Table I, along with the derived μ_{eff} values assuming a dimeric manganese unit $Mn_2(ASQ)_4(CO)_4$.

The magnetic moment per dimer at room temperature is quenched below that expected for two independent, spin-only, high-spin $3d^5$ Mn^{2+} ions (μ_s = 8.36) and below that for two high-spin $3d^6$ Mn^+ ions (μ_s = 6.93). As the temperature is lowered the moment *increases* substantially. This is indicative of a ferromagnetic exchange interaction, presumably between the pair of Mn ions. A plot of $\chi \times T$ vs. T is given in Figure 4. A simple

(25) Diebler, V. M.; Eigen, M.; Matthies, P. *Z. Naturforsch., B: Anorg. Chem., Org. Chem.* **1961**, *16B*, 629.
(26) Herberhold, M., Suss, G. *Angew. Chem., Int. Ed. Engl.* **1975**, *14*.
(27) Herberhold, M.; Wehermann, F. *J. Organomet. Chem.* **1978**, *152*, 329.
(28) Hudson, A.; Kennedy, M. J. *Inorg. Nucl. Chem. Lett.* **1971**, *7*, 333.

Table I

			calculated[a]	
T, K	χ_M(exptl)	μ_{eff}(dimer)	χ_M	μ_{eff}(dimer)
292.5	0.01190	5.28	0.01225	5.35
281.5	0.01289	5.38	0.01300	5.40
271.0	0.01382	5.47	0.01392	5.49
261.0	0.01440	5.48	0.01450	5.50
250.5	0.01541	5.55	0.01551	5.57
240.5	0.01681	5.68	0.01625	5.59
229.0	0.01767	5.69	0.01750	5.66
220.0	0.01857	5.71	0.01867	5.73
209.0	0.01986	5.76	0.02010	5.79
199.5	0.02110	5.80	0.02125	5.82

[a] Magnetic susceptibility data, least-squares fitted to $S = (3/2, 3/2)$ dimer model,

$$\chi_M = \left\{\frac{1}{T}\left[\frac{42 + 15\exp(-6J/kT) + 3\exp(-10J/kT)}{7 + 5\exp(-6J/kT) + 3\exp(-10J/kT) + \exp(-12J/kT)}\right]\right\} - \chi_0$$

best fit, $J = 23$ cm^{-1}, $\chi_0 = 0.0039$. Values for $\chi^2 = \Sigma_{i=1}^{n}(0_i - e_i)^2/e_i$ are 0.040×10^{-3} for $J = 23$ cm^{-1} and 0.50×10^{-3} for $J = 5$ cm^{-1} and $\chi_0 = 0$.

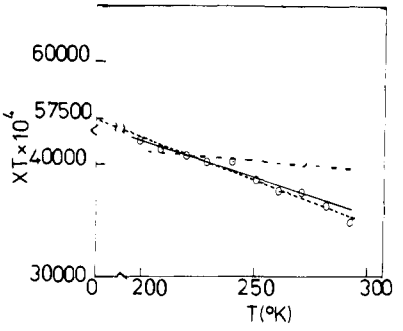

Figure 4. Plots of $\chi_M \cdot T$ vs. T. The open circles represent the experimental data and the dashed line a linear least-squares fit to the data points; (- - -) non-linear least-squares best fit to the simple dimer model described in the text with $J = 5$ cm^{-1} and $\chi_0 = 0$; (—) non-linear least-squares best fit to the dimer model with $J = 23$ cm^{-1} and $\chi_0 = 0.0039$.

Curie paramagnetic would give a horizontal straight line in such a plot. When extrapolated to $T = 0$ the limiting magnetic moment is $\mu_{eff} = 6.78$, which is slightly below the spin-only value for an $S = 3$ ground state, $\mu_s = 6.94$. The data set in Table I were confirmed on two separately prepared samples. A third data set confirmed the negative slope, but the absolute calibration was not measured.

Reaction With Oxidants. The solution dimer was oxidized with 1 equiv of the single electron oxidants Ce(IV) or $NOBF_4$ in an effort to generate the mixed-valence dimer. In both cases a deep red colored solution is formed in the presence of excess quinone in freshly distilled DME. A solution electronic spectrum run in the near-IR region did not show the band expected for an intervalence charge-transfer transition for a mixed-valence Mn cluster.

A red-brown solid is isolated from the reaction with $NOBF_4$. An EPR spectrum taken at room temperature shows the presence of a larger concentration of free Mn(II) ion that is not observed in the unoxidized dimer.

The dimer is thus unstable to one-electron oxidation in DME yielding monomeric Mn(II), presumably by oxidation of bound semiquinone followed by dissociation of the dimer.

Conductivity. AC conductivity measurements in acetonitrile showed that the solution exhibited an equivalent conductance of 6 mhos cm^2 equiv^{-1}. This is a factor of 25 below typical 1:1 strong electrolytes. The material is thus non-ionic.

Discussion

The conductivity data, infrared spectrum, chemical analysis, and mass spectrometry results provide evidence that the major photochemical product can be formulated as the electrically neutral complex $Mn_4(SQ)_4(CO)_8$·toluene. Identification of the ligand oxidation state with the semiquinone form is consistent with the electronic spectroscopy, magnetic susceptibility, and air oxidation sensitivity of the semiquinone. Magnetic susceptibility of this product is consistent with a weakly coupled antiferromagnetic cluster having a ground state that approaches diamagnetic behavior. These results can be compared with the photochemical and thermal reactions of Ni and Co carbonyls with 3,5-di-*tert*-butyl-1,2-benzoquinone (DBQ) to yield the tetrameric semiquinone complexes $[M(DBSQ)_2]_4$.[21] These are neutral complexes having the diavalent metal oxidation state. The inner coordination geometry is analogous to a chair configuration with Co and O atoms at alternating vertices. In the solid state these complexes exhibit net antiferromagnetic coupling to yield temperature-dependent moments tending toward diamagnetic ground states. The semiquinones occur as bidentate terminal ligands and as bridging ligands between metal ions. Although we have no structural data on the Mn complex, it is reasonable to assume it may have a similar structure except for the replacement of 4 DSQ terminal ligands with 8 CO ligands.

The EPR and magnetic susceptibility of the Mn complex in solution are strikingly different from the results obtained on the solid. These provide evidence for a binuclear Mn cluster having a paramagnetic ground state with $S = 3$.

Modelling of the EPR and susceptibility results was conducted by assuming an isotropic exchange interaction between a pair of spins, S_1 and S_2. This leads to a ladder of spin states having an energy given by

$$E(S;S_1,S_2) = -J[S(S+1) - S_1(S_1+1) - S_2(S_{2+1})] \quad (1)$$

This expression arises from solving the Heisenberg exchange hamiltonian, $-2J\vec{S}_1\cdot\vec{S}_2$. The total spin of the pair may adopt the values $S = S_1 + S_2, S_1 + S_2 - 1, \ldots, |S_1 - S_2|$. The sign of J determines which of these spin states is the ground state.

The EPR resonances at 10.6 K arise from transitions within the lowest of these spin states. Each spin state is susceptible to zero-field splittings. A theoretical spectrum was calculated by using the following spin Hamiltonian

$$\mathcal{H} = -2J\vec{S}_1\cdot\vec{S}_2 + D[\vec{S}_z^2 - {}^1/_3S(S+1)] + E(\vec{S}_x^2 - \vec{S}_y^2) + \beta\vec{H}\cdot\hat{g}\vec{S} + A\vec{S}\cdot\vec{I} \quad (2)$$

This includes zero-field terms for axial (D) and orthorhombic (E) distortions from cubic symmetry, g-tensor anisotropy, and isotropic hyperfine coupling (A).

It is often observed for dimeric metal complexes that the exchange term predominates in eq 2. In this limit a perturbation theory solution to eq 2 is possible by using the coupled spin states as zero-order eigenstates, $|S,M_s;S_1S_2\rangle$. A general perturbation expression for the energy (W) of these states, correct through second-order, was derived in order to determine the theoretical transitions: the result is eq 3. The X-band transitions predicted

$$\begin{aligned} W(S,M_s;S_1,S_2) = {} & -J[S(S+1) - S_1(S_1+1) - S_2(S_2+1)] + \\ & D\left[M_s^2 - \frac{1}{3}S(S+1)\right] + g_\parallel\beta H(\cos\theta)M_s + AM_IM_s + \\ & \frac{1}{2}\left\{\frac{(g_\perp\beta H\sin\theta)^2[S(S+1) - M_s(M_s-1)]}{(2M_s-1)D + g_\parallel\beta H(\cos\theta) + AM_I} \times \right. \\ & \frac{-(g_\perp\beta H\sin\theta)^2[S(S+1) - M_s(M_s+1)]}{(2M_s+1)D + g_\parallel\beta H(\cos\theta) + AM_I} - \\ & \frac{E^2[S(S+1) - M_s(M_s+1)][S(S+1) - (M_s+1)(M_s+2)]}{4[2(M_s+1)D + g_\parallel\beta H(\cos\theta) + AM_I]} \\ & \left. + \frac{E^2[S(S+1) - M_s(M_s-1)][S(S+1) - (M_s-1)(M_s-2)]}{4[2(M_s-1)D + g_\parallel\beta H(\cos\theta) + AM_I]}\right\} \end{aligned} \quad (3)$$

by this Hamiltonian were fit to the spectra given in Figure 3a,b and are shown as the stick spectrum. The inset to Figure 3a shows

the energy level splittings and the X-band transitions for one of the three canonical orientations of the magnetic field relative to the principal axes of the zero-field tensor. The assignments of the transitions in the spectrum are given in terms of the ΔM_s quantum number change. M_s is a good quantum number for the nearly axial fields found here ($E \ll D$). Six transitions are found for the $0 \leftrightarrow \pm 1$ manifold, two for each of the three canonical orientations. These peaks match up well with the six peaks observed in group III of the experimental spectrum, with the exception of the small Mn(II) impurity overlapping the central two peaks of the group. There also is predicted an apparent $\Delta M_s = 2$ "forbidden" transition at half field which matches closely transition II, and a pair of flanking $\Delta M_s = \pm 1$ transitions to higher-lying M_s states which coincide with transitions I and IV. The 11-line hyperfine structure shown in Fiugre 3b was fitted well by an isotropic coupling to two equivalent Mn nuclei $I = I_1 + I_2 = 5$. It is possible to account for the observed fine structure with a paramagnetic ground state with even spin $S \geq 2$.

The rather small zero-field splitting is further evidence for the Mn(II) oxidation state in which a high-spin electron configuration exists. Furthermore, the D and E parameters are smaller by a factor of 2 than those found in typical monomeric Mn(II) complexes. This is as expected for a dimeric structure.[29]

The experimental magnetic moment in solution clearly establishes a weak, temperature-sensitive, ferromagnetic interaction corresponding to an extrapolated value of 6.78 μ_B per $Mn_2(ASQ)_4(CO)_4$ unit at 0 K. An $S = 3$ ground state is predicted for a ferromagnetic Mn(II) dimer having four semiquinone anion radicals which are *antiferromagnetically* coupled to the Mn(II) ions, J(Mn–ASQ) < 0. The spin-only moment for this ground state is 6.94. Modelling of the susceptibility data, including explicit coupling betwen the six spins in such a complex, was not attempted. Instead, the susceptibility data were fitted to an equation derived for an $S = (^3/_2, ^3/_2)$ pair[30,31] by a non-linear least-squares fitting routine in which the exchange parameter, J, in eq 1 was found. This is tantamount to assuming that the $Mn(ASQ)_2$ unit behaves as an "effective" $S = ^3/_2$ particle over the entire temperature range. The best fit was found with a ferromagnetic interaction between the pair of $S = ^3/_2$ particles with $J = 5$ cm^{-1}. The resulting fit is poor (plotted in Figure 4). The fit was significantly improved by including a small uniform decrease (χ_0) in the susceptibility expression. This allows correction for a possible temperature-dependent J that decreases with rising T. A good fit was then found with $J = 23$ cm^{-1} and $\chi_0 = 0.0039$ (Table I). This theoretical curve is plotted in Figure 4.

To account for this temperature dependence we suggest a temperature-dependent equilibrium between the following internal redox forms (tautomers) of a discrete dimer:

$$\underset{S=3}{\underset{\text{I}}{[Mn^{II}(ASQ)_2L]_2}} \rightleftharpoons \underset{S=0 \text{ or } 3}{\underset{\text{II}}{[Mn^{III}(ASQ)(AQL)L]_2}} \rightleftharpoons \underset{S=0}{\underset{\text{III}}{[Mn^{IV}(AQL)_2L]_2}}$$

In this scheme AQL refers to the 2-acetyl-1,4-benzoquinol dianion and L refers to solvent ligand (CH_3CN or DME). The predicted electronic spin of the ground state is given below each structure. According to this scheme, structure I represents the favored tautomer at low temperature, while structures III and possibly II are favored with increasing temperature. For structure I the ASQ bridging ligands are expected to foster ferromagnetic coupling between Mn(II) ions, by a mechanism given below, and hence an $S = 3$ ground state is predicted. As the temperature is increased structures II and III are populated, and the latter of these is predicted to have an $S = 0$ ground state, owing to the closed electronic shell of the bridging AQL ligands. In II either $S = 0$ or $S = 3$ could be the ground state depending upon whether

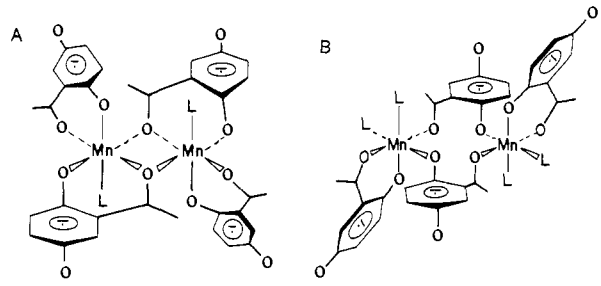

Figure 5. Proposed structures for the manganese(II,II) dimer in solution. L ≡ solvent (DME, CH_3CN) or CO.

the bridging ligands are best formulated as AQL or ASQ, respectively. This mechanism would lead to a decrease in the magnetic susceptibility with increasing temperature and so could account for the apparent temperature-dependent J needed to fit the data. Pierpont et al. have observed several examples of similar internal redox equlibrium.[32] Structure I is consistent with the weak zero-field splitting observed by EPR, but structures II and III are not. Population of low-lying excited spin states of structure I and the chemical equilibrium above contribute to the temperature dependence of the magnetic susceptibility.

The agreement observed with this model implies that antiferromagnetic interactions exist between Mn(II) and two semiquinones at low temperature. This leads to a quenching of the moment well below that for an $S = (^5/_2, ^5/_2)$ pair. Two such $Mn(ASQ)_2$ units are ferromagnetically coupled by a much weaker interaction ($J = 23$ cm^{-1}), as is indicated by EPR.

The presence of ferromagnetic coupling within simple dimeric metal complexes is an uncommon observation. This suggests a structure in which two semiquinone radicals serve to bridge the Mn(II) ions, thus enforcing a ferromagnetic Mn–Mn interaction transmitted by mutual overlap with the HOMO of the bridging semiquinones: The bridging arrangement in A is analogous to

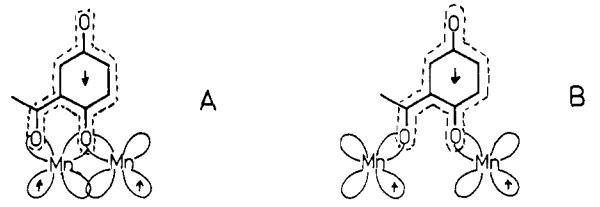

that observed in $[Co(DBSQ)_2]_4$.[21] If we adopt the bridging geometry observed for these tetrameric Ni and Co complexes with DBSQ in the solid state, then a possible solution phase structure for the dimeric Mn complex with ASQ ligands is given by Figure 5A. Another possibility is the bridging structure given in Figure 5B. These are consistent with the various experimental techniques employed in this study.

Conclusions

It has been deduced from analysis of the EPR spectrum of the photosynthetic oxygen evolving complex that ferromagnetic coupling between some of the Mn ions is present within a unit of two or four ions involving Mn(III) and Mn(IV).[5,9] The present results suggest that paramagnetic bridging ligands may transmit ferromagnetic interactions between Mn ions and so should be considered as candidates for bridging ligands in the enzyme. Suitable candidates include plastosemiquinone, paramagnetic amino acid residues such as the imidazole radical, or the intermediate oxidation products of water·OH and O_2^-. Direct evidence for the involvement of quinones in Mn coordination remains speculative. Definite evidence must await further isolation and characterization of the intact enzyme.

Acknowledgment. We thank Drs. David Hendrickson and Cortland Pierpont for preprints of their work, Drs. Steven Cooper and Jeffrey Schwartz for informative discussions, and Dr. Andrew

(29) Porte, A. L. In "Electron Spin Resonance"; P. B. Ayscough, P. B., Ed.; The Royal Society: London, 1981; Vol. 6.
(30) Earnshaw, A.; Lewis, J. *Nature (London)* **1958**, *181*, 1262.
(31) Martin, R. L. "New Pathways in Inorganic Chemistry"; The University Press: Cambridge, 1968.
(32) Pierpont, C. G.; Buchanan, R. M. *Coord. Chem. Rev.* **1981**, *38*, 45.

Bocarsly for assistance with the electrochemical measurements. We are grateful to Dr. B. C. UnniNair who kindly checked our Mn analytical data. This work has been supported by a grant from the Department of Energy/Solar Energy Research Institute (DE-FG02-80CS84003) and by an award from the Chicago Community Trust/Searle Scholars Program (G.C.D.).

Registry No. $Mn_2(AQL)_4$, 87556-35-2; $Mn_2(AQL)_4L_2$ (L = CH_3CN), 87556-36-3; $Mn_2(AQL)_4L_2$ (L = DME), 87556-37-4; 2-acetyl-1,4-benzoquinone, 1125-55-9; dimanganese decacarbonyl, 10170-69-1.

Positive Shift of Redox Potential of $[Fe_4S_4(Z\text{-cys-Gly-Ala-OMe})_4]^{2-}$ in Dichloromethane

Norikazu Ueyama, Toshitsugu Terakawa, Michio Nakata, and Akira Nakamura*

Contribution from the Department of Macromolecular Science, Faculty of Science, Osaka University, Toyonaka, Osaka 560, Japan. *Received February 22, 1983*

Abstract: $[Fe_4S_4(Z\text{-cys-Gly-OMe})_4][NMe_4]_2$ (**1**) and $[Fe_4S_4(Z\text{-cys-Gly-Ala-OMe})_4][NMe_4]_2$ (**2**) were prepared from $[Fe_4S_4(S\text{-}t\text{-Bu})_4][NMe_4]_2$ and the corresponding peptides as a model of *P. aerogenes* Fd. A positive shift in redox potential (120 mV) of **2** was observed in dichloromethane at 233 K. No shift was detected in the case of **2** in the dimethylformamide or **1** in CH_2Cl_2 even at low temperatures. The results strongly suggest that the shift of redox potential is caused by the NH---S hydrogen bond between Ala NH and Cys S in **2**. The CD spectra and IR spectra of **2** also support a peptide folding induced by the NH---S bond.

Introduction

The importance of redox potentials in biochemical electron transfer is well known, but factors controlling the redox potentials of native ferredoxins have to be elucidated. A synthetic model of 4Fe ferredoxin, e.g., $[Fe_4S_4(SCH_2Ph)_4]^{2-/3-}$, has a redox potential at −1.25 V (SCE) in DMF which is to be compared with those (e.g., −0.93 V (SCE) in Me_2SO, −0.67 V in aqueous solution for *C. pasteurianum*, −0.57 V in aqueous solution for *D. desulfuricans*) of native ferredoxin.[1-3] Holm and his co-workers[1] inferred that the value of 2−/3− couples of native ferredoxins such as *C. pasteurianum* Fd,[2] *D. desulfuricans* Fd,[3] and *C. acidiurici* Fd[3] arises principally from extrinsic protein structural effects. Their efforts in the synthesis of the peptide analogues have realized the positive shifts to some extent in $[Fe_4S_4(Ac\text{-cys-NHMe})_4]^{2-}$ [1] and $[Fe_4S_4(t\text{-Boc(-Gly-cys-Gly-)}_4NH_2)]^{2-}$,[4] which have redox potential at −0.98 V (SCE) in Me_2SO and −0.91 V (SCE) in Me_2SO, respectively. They reported that the redox potentials of those peptide complexes in Me_2SO approach that of denatured *C. pasteurianum* ferredoxin in Me_2SO. However, a redox potential difference of ca. 0.12 V between the *native* ferredoxins and the synthetic peptide analogues still exists.[1] In this paper, we show that the redox potential of native protein could successfully be reproduced in 4Fe-model complexes of Cys-containing tripeptide, Z-Cys-Gly-Ala-OMe.

There have been some speculations[5,6] on the difference of redox potentials, invoking formation of NH---S hydrogen bonds on the basis of the X-ray analysis of *P. aerogenes*[7] which has an homologous sequence to *Clostridium pasteurianum*.[8] However, Sweeny's group[9] has disputed this by the experimental facts that deuteration of the *exchangeable* amide protons involving the hydrogen bonds yields essentially no shift in the reduction potential.

We have examined the contribution of NH---S bonding to the redox potential of the synthetic 4Fe4S–peptide complexes with a *characteristic sequence* -Cys-Gly-Ala-. The sequence prefers special conformation in the protein circumstance. In this paper, we report the electrochemical behaviors of the 4Fe4S ferredoxin model complexes containing Z-L-Cys-Gly-OMe (Z = carbobenzoxy) or Z-L-Cys-Gly-L-Ala-OMe. Such a tripeptide containing a sequence Cys-Gly-Ala was selected as the characteristic sequence of *P. aerogenes* which causes the formation of the intramolecular NH---S bond[7] between the S atom of the Cys residue and to amide NH of the Ala residue. A 4Fe4S–dipeptide complex containing Cys-Gly was also examined because of its inability in intramolecular NH---S bonding as shown in Figure 1.

Experimental Section.

Preparation of Peptides. **(a) *N*-Carbobenzoxy-L-*S*-(acetamidomethyl)cysteinylglycine methyl ester (Z-Cys(Acm)-Gly-OMe)** was prepared from *N*-carbobenzoxy-L-*S*-(acetamidomethyl)cysteine and glycine methyl ester by using dicyclohexylcarbodiimide. Recrystallization of the crude compounds was carried out from methanol/ether: mp 135.6–137.0 °C (dec; $[\alpha]^{25}_D$ −22.5° (*c* 0.111, DMF). Anal. Calcd for $C_{17}H_{23}N_3O_6S$: C, 51.37; H, 5.83; N, 10.57. Found: C, 51.15; H, 5.79; N, 10.41. **(b) *N*-Carbobenzoxyl-L-*S*-(acetamidomethyl)cysteinylglycyl-L-alanine methyl ester (Z-Cys(Acm)-Gly-Ala-OMe)** was prepared from glycyl-L-alanine methyl ester and *N*-carbobenzoxy-L-*S*-(acetamidomethyl)cysteine by following the mixed anhydride method: mp 180.2–181.6 °C dec; $[\alpha]^{25}_D$ −21.6° (*c* 0.111, DMF). Anal. Calcd for $C_{20}H_{28}N_4O_7S_4$: C, 51.27; H, 6.02; N, 11.96. Found: C, 51.57; H, 6.09; N, 11.25. **(c) Z-Cys-Gly-OMe.** Cleavage of S-blocking groups was performed by the following method. To the solution of Z-Cys(Acm)-Gly-OMe (0.84 g, 2.1×10^{-3} mol) in Me_2SO were added mercury(II) chloride (1.15 g, 0.42×10^{-3} mol) and 5 mL of water at room temperature. The white precipitates obtained were collected and washed with water. The mercury(II) complex of Z-Cys-Gly-OMe was dispersed in methanol, followed by bubbling gaseous hydrogen sulfide for 15 min. After black solids were filtered off, concentration of the methanol solution under reduced pressure gave white crystals that were washed with degassed ether. **(d) Z-Cys-Gly-Ala-OMe.** The Acm group of Z-Cys(Acm)-Gly-Ala-OMe was removed by the same procedure mentioned above.

Preparation of 4Fe–4S Complexes. All 4Fe–4S complexes of Cys-containing peptides were prepared from $[Me_4N]_2[Fe_4S_4(S\text{-}t\text{-Bu})_4]$ with the ligand exchange method reported by Holm.[1,4,10] $[Et_4N]_2[Fe_4S_4(SCH_2Ph)_4]$ was prepared by the method reported by Averill et al.[11]

(1) Hill, C. L.; Renaud, J.; Holm, R. H.; Mortenson, L. E. *J. Am. Chem. Soc.* **1977** *99*, 2549.
(2) Lode, E. T.; Murray, C. L.; Rabinowitz, J. C. *J. Biol. Chem.* **1976**, *251*, 1683.
(3) Zubieta, J. A.; Mason, R.; Postgate, J. R. *Biochem. J.* **1973**, *133*, 851.
(4) Que, L., Jr.; Anglin, J. R.; Bobrik, M. A.; Davison, A.; Holm, R. H. *J. Am. Chem. Soc.* **1974**, *96*, 6042.
(5) Adman, E. T.; Watenpaugh, K. D.; Jensen, L. H. *Proc. Natl. Acad. Sci. U.S.A.* **1975**, *72*, 4854.
(6) Sheridan, R. P.; Allen, L. C.; Carter, C. W., Jr. *J. Biol. Chem.* **1981**, *256*, 5052.
(7) Adman, E. T.; Sieker, L. C.; Jensen, L. H. *J. Biol. Chem.* **1973**, *248*, 3987.
(8) Tanaka, M.; Nakashima, T.; Benson, A. M.; Mower, H. F.; Yasunobu, K. T. *Biochemistry*, **1966**, *5*, 1666.
(9) Sweeney, W. V.; Magliozzo, R. S. *Biopolymers* **1980**, *19*, 2133.
(10) Bobrik, M. A.; Que, L., Jr.; Holm, R. H. *J. Am. Chem. Soc.* **1974**, *96*, 285.

0002-7863/83/1505-7098$01.50/0 © 1983 American Chemical Society